Received: 27 June 2025 | Revised: 26 August 2025 | Accepted: 9 September 2025

DOI: 10.1002/aic.70083

AIChE JOURNAL

RESEARCH ARTICLE

Reaction Engineering, Kinetics and Catalysis

Harnessing structured coke in zeolites to boost ethylene yield in methanol-to-olefins by low-temperature regeneration

Guida Li[1,2] | Jinling Zhang[2] | Shanfan Lin[2] | Yuhan Song[2] | Hua Li[2] | Wenjie Peng[2] | Hanlixin Wang[3] | Zhaochao Xu[3] | Yingxu Wei[2] | Mao Ye[1,2] | Zhongmin Liu[2]

[1]Department of Chemical Physics, University of Science and Technology of China, Hefei, China

[2]National Engineering Research Center of Lower-Carbon Catalysis Technology, Dalian Institute of Chemical Physics, Chinese Academy of Sciences, Dalian, China

[3]Key Laboratory of Separation Science for Analytical Chemistry, Dalian Institute of Chemical Physics, Chinese Academy of Sciences, Dalian, China

Correspondence
Mao Ye, National Engineering Research Center of Lower-Carbon Catalysis Technology, Dalian Institute of Chemical Physics, Chinese Academy of Sciences, Dalian, 116023, China.
Email: maoye@dicp.ac.cn

Funding information
National Natural Science Foundation of China, Grant/Award Numbers: 22293021, 22288101

Abstract

In industrial zeolite catalysis, high-temperature (>650°C) air combustion is commonly used to restore the activity of catalysts deactivated by coke deposition. Herein, we propose a low-temperature (440–500°C) air regeneration strategy that harnesses spatially restructured coke in SAPO-34 catalysts for enhanced performance in the methanol-to-olefins reaction. The resulting "tight-outside, loose-inside" coke distribution expands accessible reaction volumes, improves product transport, and enhances exposure of confined naphthalene species, key intermediates for ethylene formation. Compared to conventional high-temperature air regeneration that substantially removes coke, the proposed strategy repurposes it as a functional promoter, enabling prolonged catalyst lifetime and markedly improved ethylene selectivity. The practical viability of this strategy was further confirmed by pilot-scale fluidized bed reactor-regenerator experiments and process simulations in terms of both catalyst stability and thermal utilization efficiency. This work reveals an alternative approach to enhance shape-selective zeolite catalysis via rationally modulating coke by controlling the regeneration strategy.

KEYWORDS
coke spatial distribution, low-temperature regeneration, methanol-to-olefins, molecule diffusion, SAPO-34 zeolite

1 | INTRODUCTION

Zeolite catalysts, owing to their distinctive structures, favorable micro-environment, and excellent shape selectivity, have been widely used in industrial processes that convert oil- and/or coal-based feedstocks into a variety of fuels and chemicals.[1–3] One of the big challenges in zeolite-catalyzed industrial processes, including fluid catalytic cracking (FCC), methanol-to-olefins (MTO), and others, is the rapid deactivation of catalysts due to the deposition of coke species, that is, heavy aromatic molecules, in zeolites.[4–8] The coke species would cover the active sites or block the nanopores within zeolite crystals, significantly reducing catalytic activity and product yield. A common regeneration practice is air combustion of the deposited coke in order to recover zeolite catalyst activity and maintain continuous industrial operation.[9–11] Normally, catalyst regeneration in industrial processes is carried out at a temperature higher than 650°C to enhance the combustion rate and promote regeneration capability.[9,12] However, the presence of zeolite catalysts in a high-temperature steam environment inevitably induces irreversible hydrolysis of Si–O–Al bonds, resulting in partial framework collapse and structural degradation.[13–15] Air combustion of coke deposited in zeolites at such high temperatures compromises hydrothermal stability and thus shortens the lifespan of zeolite catalysts as the flue gas is essentially steam-containing.[16–18] Developing an effective regeneration strategy which can alleviate the

hydrothermal stress and at the same time maintain comparable efficacy in removing coke species and restoring catalyst activity is of practical importance for zeolite catalysis such as MTO.

It is widely accepted that the MTO reaction operates via a dynamic autocatalytic hydrocarbon pool (HCP) mechanism, wherein active intermediates such as polymethylbenzenes and the corresponding carbenium ions orchestrate a multi-cycle network for efficient olefins generation.[3,19,20] The coke species, typically polyaromatics, are formed in MTO as a result of gradual transformation of HCP species. Essentially, coke not only causes catalyst deactivation but also imposes shape-selective constraints that modulate product selectivity.[21–24] This dual role of coke, as both a deactivating agent and a selectivity mediator, has stimulated industrial practices such as pre-coking and controlled incomplete regeneration to maintain optimal coke levels for maximizing light olefins yields.[25–28] Removing coke deposited in spent catalyst in the aforementioned practices, however, still relies on high-temperature air combustion. A recently emerging steam cracking technique, which converts inactive species to active naphthalene intermediates in molecular sieves, can simultaneously enhance ethylene selectivity and produce valuable flue gas components, highlighting its potential to replace conventional air regeneration methods. A constraint for this technique, however, is that the steam cracking of coke species takes place at an even higher temperature (650–700°C) in the presence of a large fraction of steam.

In this work, we, for the first time, propose a low-temperature regeneration strategy based on air combustion at a temperature of 440–500°C for MTO over an industrially significant SAPO-34 zeolite catalyst. This proposal builds our understanding of the mechanistic intricacies of the MTO process and the multifaceted role of coke in catalysis. Importantly, we found that the moderated decoking kinetics at low temperature enable the formation of a more favorable coke distribution within the zeolite crystals, which in turn facilitates methanol conversion and promotes the diffusion of light olefin products. In addition to the expected enhancement of hydrothermal stability in the industrial MTO process, this strategy also leads to a notable elevation of ethylene selectivity and catalyst lifespan, while effectively restoring catalytic activity. The practical viability of this strategy was confirmed by pilot-scale fluidized bed reactor-regenerator experiments and process simulations in terms of both catalyst stability and thermal utilization efficiency. Crucially, the proposed low-temperature regeneration technique might mitigate the limitations of current high-temperature air regeneration in precisely controlling combustion temperature and coke content distribution within the regenerator, thereby holding significant potential for enhancing the MTO process.[9,11]

2 | METHODS SECTION

2.1 | Catalysts and their structural characterizations

The catalyst particles used in the microfluidized bed reactor primarily comprise SAPO-34 molecular sieve as the active component, along with adhesives and other dispersed components within the matrix, which were procured from Catalyst & Catalysis Technology Co. Ltd. of Chinese Academy of Sciences (CAS). The SAPO-34 molecular sieve crystals with an average particle size of 6 μm used for structured illumination microscopy (SIM) were purchased from Tianjin Yuanli Chemical Co., Ltd. Phase structural information and the microscopic morphology of these catalysts were characterized using PANalytical X'Pert PRO x-ray X-ray diffraction (XRD) and scanning electron microscope (SEM, Hitachi SU8020), as depicted in Figures S1 and S2. The Brunauer-Emmett-Telle (BET) surface area and micropore volume of all catalysts (including fresh, deactivated, and partially regenerated) were measured through nitrogen physical adsorption–desorption experiments at 77 K using a Micromeritics ASAP 2020 analyzer.

2.2 | Catalytic reaction and air regeneration treatment

In this experiment, the preparation of deactivated catalysts and the evaluation of regenerated catalysts for the MTO reaction were performed in a microfluidized bed reactor with an inner diameter of 19 mm. Prior to the reaction, the selected catalyst particles, ranging from 80 to 120 mesh in size, were pre-treated in a muffle furnace at 600°C for 6 h to remove the organic template for unblocking the pores. Subsequently, 3.0 g catalysts were introduced into the microfluidized bed, and at 470°C under atmospheric conditions, the reaction mixture of methanol and water (in a 4:1 mass ratio) was pumped into the tube at a weight hour space velocity (WHSV) of 2 $g_{MeOH}\ g_{CAT}^{-1}\ h^{-1}$. Fresh catalysts were activated at 500°C for 30 min under a nitrogen atmosphere before coming into contact with methanol, following which they are then cooled to the desired temperature for the MTO reaction. When the methanol conversion drops below 80%, the catalyst is considered inactive.

The deactivated catalysts were introduced into either a microfluidized bed reactor or a fixed bed reactor with a 4 mm inner diameter, and heated under a nitrogen atmosphere to target temperatures of 440, 470, 500, and 600°C. Subsequently, air was introduced for varying reaction durations, at an air weight hourly space velocity (WHSV) of approximately 2 h^{-1} for the fluidized bed and 4 h^{-1} for the fixed bed. The distribution of gaseous effluent products was calculated on a CH2 basis, using methanol and DME as reactants, by using an online Agilent 7890 gas chromatography with a PLOT-Q capillary column and flame ionization detector.

2.3 | Identification of types and quantification of carbonaceous deposits

The overall coke content of deactivated and partially regenerated catalysts was measured using a thermogravimetric analyzer (TGA) performed on a TA SDTQ 600 analyzer: 10 mg of the sample was loaded into an alumina crucible and heated from room temperature to 900°C

at a rate of 10°C min^{-1} in an airflow of 100 mL min^{-1}. The weight loss within the 300–900°C range as a percentage of the net catalyst weight was calculated as the coke content.

The chemical composition of carbonaceous deposits within molecular sieve cages and those extending across cages was analyzed through gas chromatography–mass spectrometry (GC–MS, Agilent 7890A/5975C) and matrix-assisted laser desorption ionization Fourier-transform ion cyclotron resonance (MALDI FT-ICR) MS, respectively. Initially, 20 mg of coked and regenerated catalysts was dissolved in 1 mL of 10% hydrogen fluoride (HF) to dissolve the framework and release carbonaceous species. Subsequently, extraction was conducted using dichloromethane containing 100 ppm of hexachloroethane as an internal standard, and the lower organic phase was separated through liquid–liquid extraction. These extraction phases were introduced into a GC–MS fitted with an HP-5 column and a flame ionization detector (FID) detector, and the species composition was ultimately identified by matching against the National Institute of Standards and Technology (NIST) database. MALDI FTICR MS can provide carbonaceous species with molecular weights ranging from 150 to 2000 Da, complementing the limited information provided by GC–MS. The extracted organic phase was blended with a 1,8,9-anthracenetriol (dithranol) matrix, and then 1 μL of this mixture was applied to the sample holder for drying, and was introduced into the ion source of the mass spectrometer for analysis. The 15-T FT-ICR MS (Bruker Daltonics, Bremen, Germany) is equipped with an Nd:YAG laser emitting a 355 nm laser to ionize molecules, and employs a reflection-mode time-of-flight mass analyzer to record the MS signals.

The quantitative analysis of coke species, including oxygen-containing species grown within cages was determined by the internal standard method. Toluene, phenanthrene, and 1*H*-Phenalen-1-one (PO) were chosen as model compounds to represent light carbonaceous deposition. A series of standard solutions containing different concentrations of model compounds with a 100 ppm internal standard were prepared and analyzed via GC–MS to determine the mass correction factors for the FID signal integration area of these species.[29] The resulting standard curve is depicted in Figure S34, with the horizontal axis showing the area ratio of the test species to the internal standard (A_i/A_{std}), and the vertical axis indicating the concentration of the test species. The mass of larger heavy carbonaceous deposits grown spanning multiple cages is determined by subtracting the mass of light deposits within the individual cages from the total coke content measured by TGA.

The evolution of chemical bond information for coke species in deactivated catalysts under an air atmosphere was recorded using *in situ* diffuse reflectance infrared Fourier-transform (DRIFT) spectroscopy on a Bruker Tensor 27 device, which was equipped with a diffuse reflector and mercury cadmium telluride (MCT) detector. SAPO-34 molecular sieve crystals, containing varying levels of coke after being regenerated at different temperatures, were subjected to Raman spectroscopy using a 405 nm excitation source to monitor changes in Raman signals at the crystal scale. A 100× long working distance objective lens (Olympus, 0.5 NA) was employed to focus on the sample surface, while ensuring that the laser power remained below 2 mW to preserve the integrity of the molecular sieve samples. Spectral acquisition on the molecular sieve crystals occurred at a frequency of approximately 6 s, covering a wavelength range of 50–2500 cm^{-1}.

2.4 | Isotope labeling experiment of ^{13}C-methanol

The regenerated catalysts, still containing a specific amount of coke, were placed in a fixed bed reaction tube with an inner diameter of 4 mm and activated for 30 min under a nitrogen atmosphere at 500°C. Subsequently, the temperature was reduced to 470°C, and ^{13}C labeled methanol, with a WHSV of 2 g_{MeOH} g_{CAT}^{-1} h^{-1}, was introduced into the reaction tube via nitrogen carrier gas at a specific flow rate. The reaction was sustained for durations of 30 s and 10 min. Immediately upon completion of the reaction, the ^{13}C-methanol feed was discontinued, and the catalysts were quenched with liquid nitrogen. Finally, the isotopic distribution of coke species within the catalyst was analyzed using the mentioned dissolution-extraction method.

2.5 | Structured illumination microscopy

SIM is capable of acquiring super-resolution images depicting the spatiotemporal distribution of coke species with varying concentrations following air regeneration. Super-resolution imaging was conducted with the Nikon N-SIM super-resolution microscope system, which includes an electric inverted microscope ECLIPSE Ti2-E, a 100×/NA 1.49 oil-immersed total internal reflection fluorescence (TIRF) objective (CFI HP), and an ORCA Flash 4.0 s CMOS camera (Hamamatsu Photonics K.K.). Imaging was carried out with multi-laser sources at 405, 488, 561, and 640 nm, with excitation emissions captured by four photomultiplier tubes within the ranges of 435–485, 500–545, 570–640, and 663–738 nm, respectively. The acquired images were analyzed with NIS Elements Ar and N-SIM Analysis software, and super-resolution images were reconstructed through computational processes.

2.6 | Intelligent gravimetric analyzer

The uptake isotherms of methanol and propane were determined on a high-precision intelligent gravimetric analyzer (IGA) (IGA100, Hiden Isochema Ltd., Warrington, UK). Prior to sorption measurements, approximately 20 mg of samples were loaded into the microbalance bucket and outgassed at 300°C under a vacuum of less than 10^{-6} mbar for over 4 h. The sample temperature was regulated to within 0.1°C by a furnace. Once the sample quality stabilizes, the pretreatment is considered complete. To facilitate thorough contact between the gas in the system and the catalyst sample, a mesh sample

cell is chosen. Adjust the reaction system temperature to the target levels of 25°C for methanol and 30°C for propane. Conduct gas adsorption experiments under the specified pressures of 0.6 mbar for methanol and 5 mbar for propane. Record the catalyst's mass change over time until it stabilizes, indicating system equilibrium, before advancing to the next step. It is essential to eliminate the effects of external diffusion during this experimental procedure to ensure the catalyst's quality does not influence the adsorption experiment results.

3 | RESULTS AND DISCUSSION

3.1 | MTO reaction over low-temperature regenerated catalyst

To address the challenge of rapid deactivation of SAPO-34 molecular sieve-based catalysts in the MTO process, a fluidized bed regenerator typically burning coke deposits with air at a high temperature over 650°C is connected to the reactor for *in situ* restoring catalyst activity. Such a high regeneration temperature is chosen to boost the air combustion rate and enhance regeneration capability. In real practices, however, this could pose a potential hydrothermal stability issue as the flue gas is basically steam-containing. Furthermore, air regeneration at high temperature over 650°C might also indiscriminately eliminate both active and inactive coke because of the rapid combustion rate (Figure S3), and eventually lead to the loss of original "active sites."

In this work, deactivated samples were first prepared by subjecting commercially available SAPO-34 catalysts to a microfluidized bed reactor for MTO reaction under industrial conditions (see Figure S4 for the typical product distribution). Subsequently, the deactivated catalysts were then regenerated in air at varying temperatures to investigate the changes in MTO performance. Although lowering the regeneration temperature prolongs the regeneration time required, progressive coke removal restores activity and extends lifetime, thereby demonstrating that effective regeneration can be achieved within the low temperature range of 440–500°C (Figures S5–S8). As can be seen, the decline in coke content would result in a decrease in initial olefins selectivity for the regenerated catalyst in MTO reaction, further highlighting the dual role of coke. The trade-off between catalytic lifespan and selectivity of light olefins that is typical of conventional high-temperature air combustion is somewhat mitigated under low-temperature conditions. A detailed observation shows that the

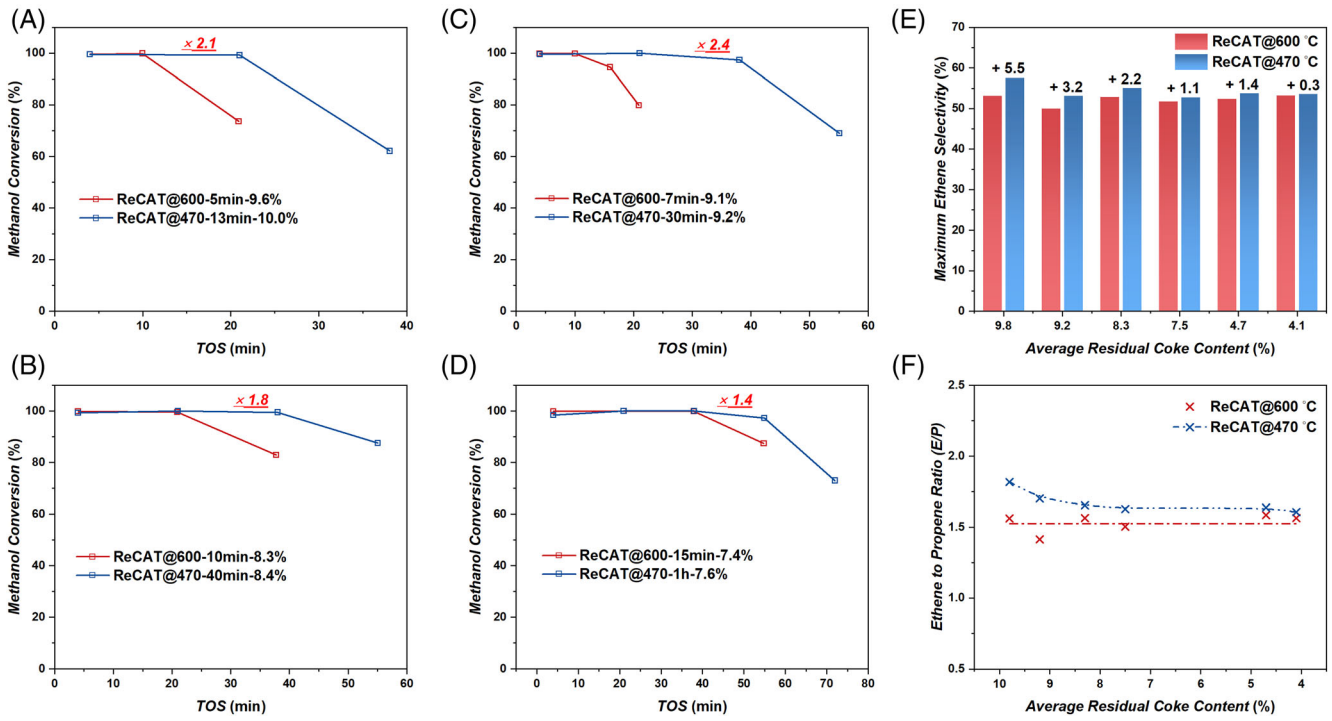

FIGURE 1 Performance metrics of partially regenerated catalysts in the methanol-to-olefins (MTO) reaction, including catalyst lifetime, maximum ethylene selectivity, and ethylene-to-propylene (*E*/*P*) ratio. Deactivated catalysts were subjected to air regeneration at different temperatures and subsequently evaluated under standard MTO conditions. (A–D) Time-on-stream methanol conversion profiles comparing catalysts regenerated at 600 and 470°C with similar coke contents, highlighting differences in catalyst lifetime. (E) Maximum ethylene selectivity and (F) *E*/*P* ratio were extracted from product distributions at various time points (see Figures S5 and S7). MTO reactions were performed at 470°C with a weight hourly space velocity (WHSV) of 2 $g_{MeOH}\ g_{cat}^{-1}\ h^{-1}$ and a methanol/water mass ratio of 4:1. Regeneration was carried out in air at either 600 or 470°C with WHSV of 4 $g_{air}\ g_{cat}^{-1}\ h^{-1}$. All experiments were conducted in a microfluidic reactor. The notation "ReCAT@600–5 min-9.6%" denotes shaped catalyst regenerated at 600°C for 5 min with a post-regeneration coke content of 9.6%, with similar interpretations applying to other notations.

catalysts regenerated at 470°C exhibit a remarkable extension of lifespan in MTO reaction, surpassing that of catalysts regenerated at 600°C by up to 2.4 times (Figure 1A–D). Additionally, it also demonstrates higher ethylene selectivity and an elevated ethylene-to-propylene ratio (Figure 1E,F). A marked increase in ethylene selectivity was observed, accompanied by a decrease in propylene selectivity, while the total light olefin selectivity showed only a slight increase. Overall, across a wide range of coke contents, regeneration at 470°C enhanced both ethylene selectivity and the ethylene-to-propylene ratio, with the improvement being particularly pronounced at relatively high residual coke levels. Further comparisons with other low-temperature regeneration conditions (440 and 500°C) reveal that regeneration at 440°C yields comparable but slightly inferior results compared to that at 470°C, while regeneration at 500°C fails to achieve a discernible improvement (Figures S10 and S11). These findings collectively underscore that low-temperature air regeneration at 470°C is not only feasible but also superior to conventional high-temperature methods in terms of both catalyst longevity and product selectivity under coke-rich conditions.

3.2 | Spatial distribution of coke species in low-temperature regenerated catalyst

The transition from high to low-temperature regeneration is accompanied by a shift in the decoking kinetics, evolving from an approximately constant rate to a progressively declining one (Figure S12). This trend is further reflected in an increasing reaction order with respect to coke content (Figure 2A), indicating a growing dependence of the regeneration process on the amount and nature of carbonaceous deposits. This behavior can be attributed to the coexistence of multiple coke species, including both light and heavy fractions (Figure S13). More detailed quantitative analysis of coke revealed that, at 600°C, both heavy and light coke components are removed

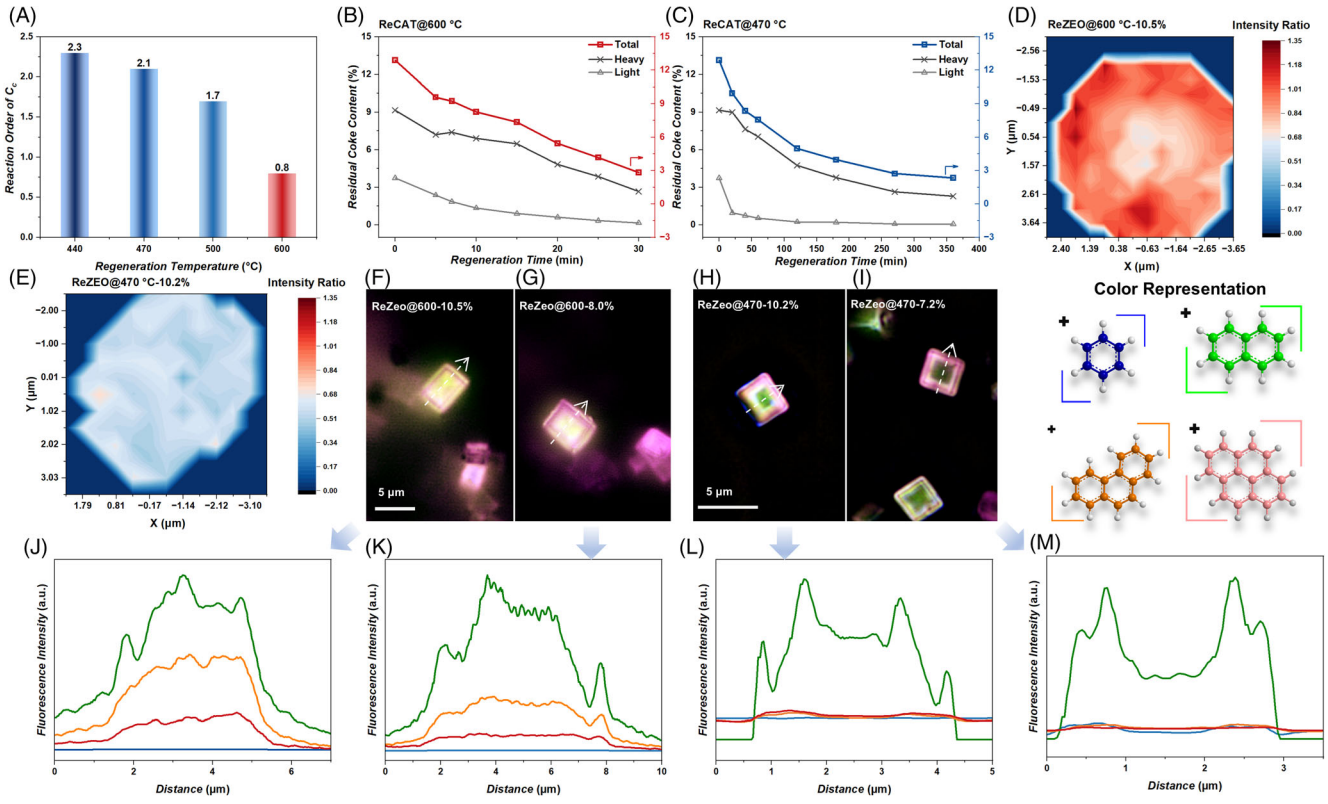

FIGURE 2 Comparative analysis of decoking behavior at both the catalyst particle and single-crystal levels. (A) Apparent reaction order with respect to coke content as a function of regeneration temperature, derived from kinetic analysis of air regeneration experiments. (B, C) Evolution of light and heavy carbonaceous species (Figure S13) during regeneration at 600 and 470°C, respectively, characterized by thermogravimetric analysis. (D, E) Spatial distribution of the Raman D-band to G-band intensity ratio within single zeolite crystals regenerated at 600°C (ReZEO@600-10.5%) and 470°C (ReZEO@470-10.2%), reflecting differences in coke structure. (F–I) Super-resolution fluorescence images (SIM) of individual zeolite crystals after regeneration at varying coke contents and temperatures: ReZEO@600-10.5%, ReZEO@600-8.0%, ReZEO@470-10.2%, and ReZEO@470-7.2%. (J–M) Corresponding fluorescence intensity profiles along selected line scans in panels (F–I). SIM imaging was performed using four excitation/emission channels: 405 nm (435–485 nm, blue), 488 nm (500–545 nm, green), 561 nm (570–640 nm, orange), and 640 nm (663–738 nm, red), with false-color representation. All zeolite crystals were first deactivated in the methanol-to-olefins (MTO) reaction and subsequently regenerated in air. The MTO reaction was conducted at 470°C with a weight hourly space velocity (WHSV) of 2 $g_{MeOH}\ g_{cat}^{-1}\ h^{-1}$ under N_2 flow. Regeneration was performed at 470 or 600°C with WHSV of 4 $g_{air}\ g_{cat}^{-1}\ h^{-1}$. The notation "ReZEO@600-10.5%" denotes a zeolite regenerated at 600°C with a post-regeneration coke content of 10.5%, with similar interpretations applying to other notations.

simultaneously. In contrast, as the regeneration temperature decreases, their removal rates become decoupled: light coke is eliminated relatively quickly, whereas heavy coke is removed much more slowly (Figures 2B,C and S14). This unmatched elimination behavior was further investigated using Raman spectroscopy (a powerful tool for characterizing carbonaceous materials[30–32]). Despite fluorescence interference, visible-light excited Raman spectra (Figures S15 and S16) successfully capture the characteristic vibrational modes of coke species confined within the zeolite framework during air regeneration.

The evolution of coke properties on catalyst crystals during regeneration at 600 and 470°C differs markedly (Figures 2D,E and S17). In the early stage of regeneration, catalysts treated at 600°C exhibit relatively higher *D*/*G* intensity ratios across the entire crystal, indicative of a larger fraction of less graphitized, lighter coke species. In contrast, regeneration at 470°C results in zeolite crystals uniformly coated with coke of lower *D*/*G* ratios, corresponding to more graphitized, heavier carbon deposits. These observations highlight the temperature-dependent reactivity of oxygen toward different coke types: at high

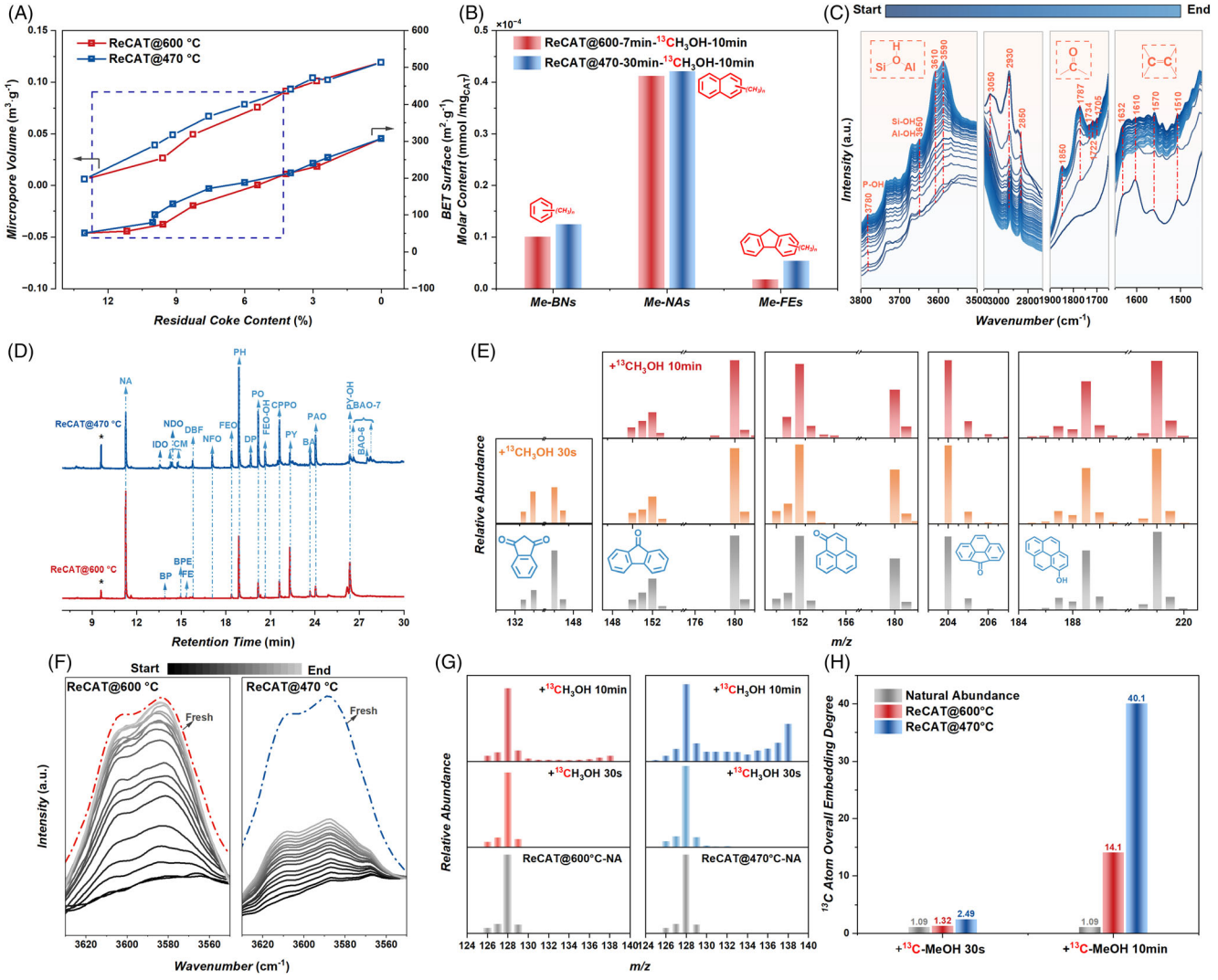

FIGURE 3 Evolution of catalyst textural properties, coke species, and results from isotopic labeling studies. (A) Changes in textural properties of the catalyst as a function of decreasing coke content during air regeneration at 600 and 470°C. (B) Absolute concentrations of polymethylbenzenes, naphthalene, and fluorene detected after a 10 min methanol-to-olefins (MTO) reaction using ^{13}C-methanol, following regeneration at 600°C for 7 min and 470°C for 30 min. Quantification assumes these aromatics originate exclusively from ^{13}C-methanol conversion. (C) *In situ* diffuse reflectance infrared Fourier-transform (DRIFT) spectra illustrating the evolution of surface species during regeneration at 470°C. (D) Gas chromatography–mass spectrometry identification of confined aromatic species remaining within zeolite cages after regeneration at 600 and 470°C (see Table S1 for molecular structures and abbreviations). (E) Representative mass spectral patterns (focusing on ions adjacent to the molecular ion) of selected oxygenated compounds before (bottom) and after (middle and top) reaction with ^{13}C-methanol (full spectra in Figure S24). (F) Recovery of Brønsted acid sites on deactivated catalysts, monitored by in situ DRIFT during regeneration at 600 and 470°C. (G) Mass spectral profiles of naphthalene species regenerated at 600 and 470°C, before (bottom) and after reaction with ^{13}C-methanol for 30 s (middle) and 10 min (top). (H) Overall embedding degree of ^{13}C atoms within individual naphthalene molecules in regenerated samples at 600 and 470°C. All MTO reactions were conducted at 470°C in a fixed-bed reactor with a weight hourly space velocity of 2 g_{MeOH} g_{cat}^{-1} h^{-1}. The use of ^{13}C-labeled methanol enables differentiation between newly formed and residual carbon species.

temperatures, coke is removed in a relatively uniform, heavy-to-light sequence (Figure S18),[33,34] whereas at low temperatures, oxygen preferentially oxidizes lighter coke species, leaving behind more refractory, heavy coke. Nonetheless, irrespective of regeneration temperature, both strategies ultimately leave behind persistent, oxidation-resistant carbon species—predominantly located in the crystal interior (Figure S17).

Furthermore, the influence of regeneration temperature on the spatiotemporal evolution of light coke species can be directly visualized via SIM.[27,28,35,36] In contrast to the relatively uniform fluorescence observed in fully deactivated zeolites (Figure S19a), two distinct spatial depletion patterns of light polycyclic aromatic hydrocarbons (PAHs) emerge under high and low-temperature oxidative conditions. At 600°C, the early stage regeneration (Figure 2F,G,J,K) is characterized by a bell-shaped intensity profile with a bright central region in the center of zeolites, indicative of a classical shrinking-core mechanism in which coke is combusted progressively from the external surface inward. In contrast, during regeneration at 470°C, the heavier cross-linked coke species are mainly distributed on the periphery of the zeolite crystals, allowing oxygen to penetrate into the crystal interior and preferentially oxidize the lighter coke located inside. As a result, the fluorescence intensity profile of coke species exhibits a concave distribution (Figure 2H,I,L,M). As regeneration progresses, both systems exhibit a gradual convergence in coke distribution profiles (Figure S19). Notably, naphthalene consistently exhibits the highest content regardless of temperature, highlighting its stability, as corroborated by the previous analysis.[27] The heterogeneity in coke composition, coupled with the temperature-dependent oxidation behavior, gives rise to marked differences in the spatial distribution of residual carbon. Essentially, the reduction in temperature reduces oxygen's ability to uniformly combust coke, resulting in a more pronounced "hollow" carbon deposition pattern at 470°C, which endows regenerated catalysts with a longer lifespan and higher ethylene selectivity compared to those regenerated at 600°C. The subsequent section will delve into the underlying causes of the enhanced MTO performance attributed to this spatial configuration.

3.3 | Accessibility of active species in low-temperature regenerated catalyst

As previously discussed, the spatial configuration of residual coke formed under low-temperature regeneration plays a critical role in enhancing MTO catalytic performance. Unlike conventional high-temperature regeneration, selective combustion at 470°C preferentially removes light coke species, resulting in a significant restructuring of the accessible pore space. As shown in Figures 3A and S20, catalysts regenerated at 470°C exhibit higher specific surface area and restored micropore volume. The expanded porosity facilitates greater methanol conversion (i.e., prolonged catalyst lifetime) and accommodates a greater amount of newly formed coke. Specifically, after identical durations of exposure to ^{13}C-methanol, catalysts regenerated at 470°C generated higher levels of ^{13}C-labeled polymethylbenzenes, naphthalene, and fluorenes than their 600°C counterparts (Supplementary Note 1.1, Figure 3B).

To elucidate the origin of enhanced ethylene selectivity, we focused on the role of catalytically active species regenerated under different conditions. *In situ* DRIFT spectroscopy was employed to monitor the evolution of surface species during regeneration (Figure 3C). Upon regeneration, characteristic OH vibrational bands (~3610 and 3590 cm^{-1}) re-emerged, indicating progressive restoration of Brønsted acid sites, alongside the appearance of various C=O functional groups (~1850 and 1700–1800 cm^{-1}) and the gradual attenuation of PAH-related C–H signals (~3050, 2930, and 2870 cm^{-1}).[37–39] Complementary GC–MS analysis after dissolution-extraction further confirmed the generation of oxygenated species, such as ketones, lactones, and anhydrides, in the regenerated catalysts (Table S1, Figures S21 and S22). While the chemical identities of these oxygenates are largely consistent across temperatures (Figure 3D), their relative abundances within light coke were significantly higher at 470°C (Figure S23). Intuitively, it can be hypothesized that the higher relative content of oxygen-containing compounds could contribute to enhancing ethylene selectivity. However, ^{13}C-methanol tracing experiments revealed that these oxygenates did not undergo carbon exchange reactions within their frameworks (Supplementary Note 1.1, Figures 3E, S24, and S25), suggesting that oxygenates are catalytically inert with respect to ethylene formation.

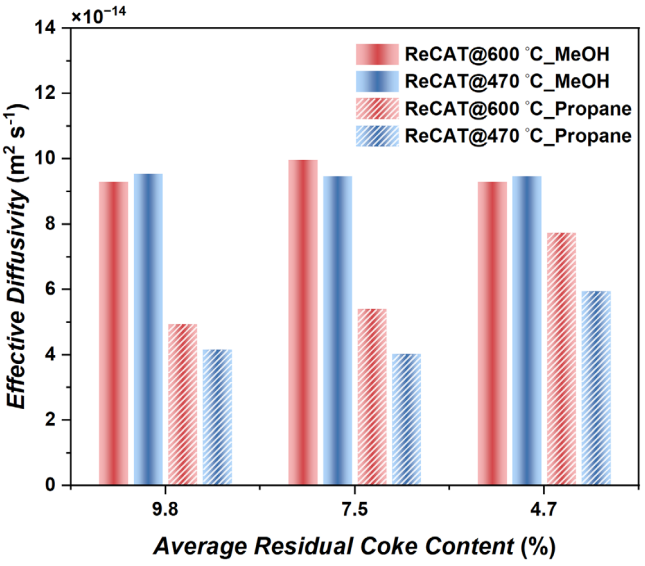

FIGURE 4 Effective diffusion coefficients of methanol and propane on catalysts with varying residual coke contents. Diffusion coefficients of methanol (measured at 25°C and 0.6 mbar) and propane (30°C and 5 mbar) were quantitatively determined via mathematical modeling for three pairs of regenerated catalysts with similar coke contents: ReCAT@470 to 13 min to 10.0% vs. ReCAT@600 to 5 min to 9.6%; ReCAT@470 to 1 h to 7.6% vs. ReCAT@600 to 15 min to 7.4%; ReCAT@470 to 2 h to 4.5% vs. ReCAT@600 to 22 min to 4.8%. The data reveal the influence of regeneration temperature and coke morphology on molecular diffusion behavior within the microporous framework.

The distinct coke distribution profiles governed by oxidation capacity modulate catalyst longevity, and should contribute to the enhancement of ethylene selectivity through accessible active species. Although low-temperature regeneration yields a lower total amount of naphthalene (Figure S26a), its spatial distribution may be more favorable for reaction and diffusion, namely, more readily interacting with methanol because of the limited restored acid sites (Figure 3F). ^{13}C-methanol labeling revealed that naphthalene behaves as a catalytically active species, undergoing carbon incorporation reactions that are absent in oxygen-containing species (Supplementary Note 1.1, Figure 3G). During the early stages of ^{13}C-methanol conversion, the 600°C-regenerated samples exhibit a ^{13}C overall embedding degree (OED) of 1.32%—close to natural abundance—compared to 2.49% for the 470°C sample. Upon extended reaction time, this value rises to 14.1% for the 600°C sample, but remains markedly lower than the 40.1% observed for the 470°C-regenerated catalyst. Furthermore, ^{13}C atom incorporation within the naphthalene molecule was more extensive and widespread in the low-temperature regenerated sample (Figure 3G,H). The pronounced ^{13}C incorporation into naphthalene directly correlates with enhanced ethylene selectivity.

The coking process within SAPO-34 crystals enhances the diffusion of light olefins,[24,40] while the spatial distribution of residual coke during the decoking process inevitably affects product selectivity by introducing mass transfer limitations. This section examines the diffusion behavior of methanol and propane as adsorbates on catalysts with varying residual coke content. Previous findings suggest that lower regeneration temperatures promote a platform-like arrangement of naphthalene and an increased accumulation of peripheral heavy deposits, thereby altering molecular motion trajectories. To analyze diffusion, a single-resistance mass transfer model—excluding surface barriers at crystal interfaces—is employed for spherical catalyst particles (Supplementary Note 1.2 for details). As illustrated in Figure 4, the effective diffusion coefficient of methanol remains

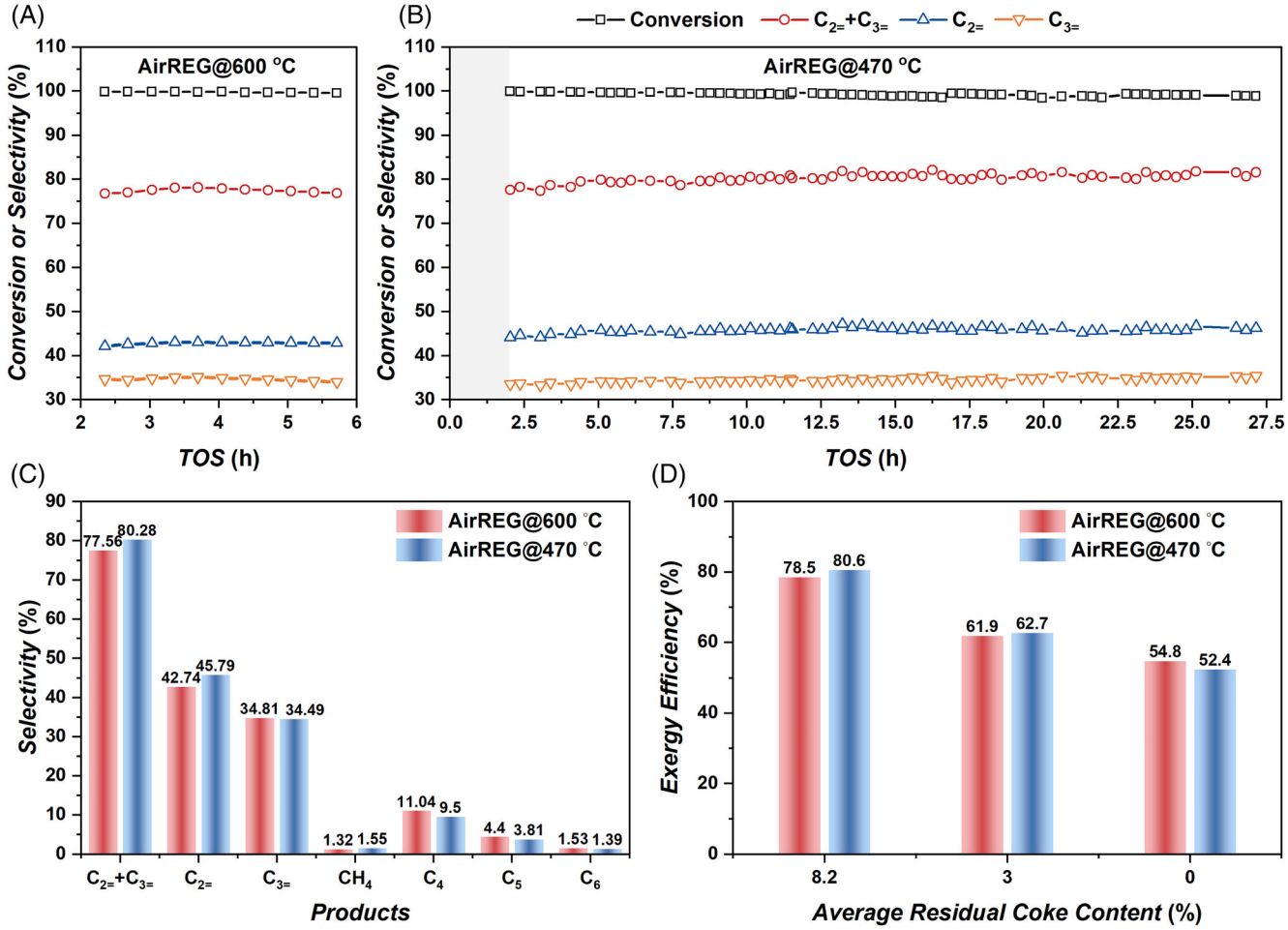

FIGURE 5 Pilot-scale evaluation and process exergy analysis of the low-temperature air regeneration strategy. (A, B) The stability test of catalysts regenerated at 600 (AirREG@600) and 470°C (AirREG@470) in a pilot-scale fluidized bed reactor-regenerator setup during the methanol-to-olefins (MTO) reaction (the initial 2 h were a pretreatment stage for preparing the deactivated catalyst without cycling). (C) Comparison of average product selectivities in MTO reactions using catalysts regenerated at 470°C (AirREG@470) and 600°C (AirREG@600). (D) Exergy analysis of the regeneration system under three simulated regeneration scenarios, performed using ASPEN Plus. Pilot-scale reaction conditions: Reaction temperature of 470°C, regeneration temperatures of 470 and 600°C (average coke content of 4.3% and 5.3%, respectively), weight hour space velocity of 2 g_{MeOH} g_{cat}^{-1} h^{-1}, catalyst circulation rate of 680 g h^{-1}, and total catalyst inventory of 5 kg.

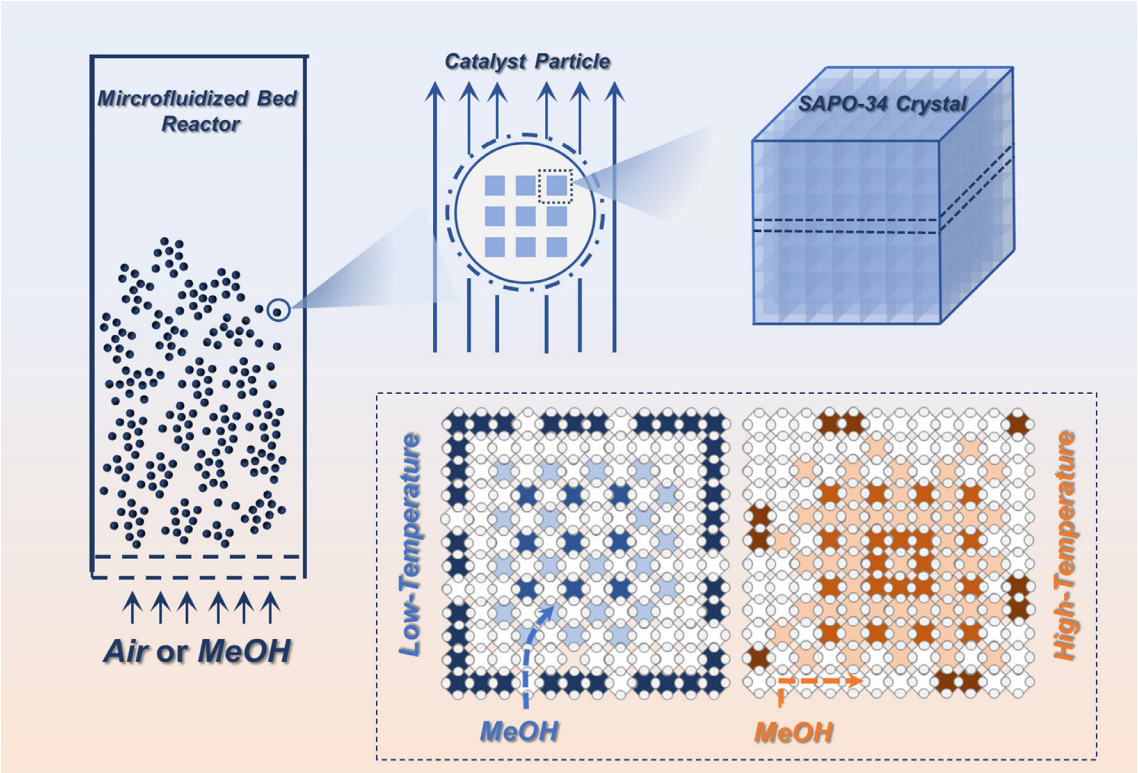

SCHEME 1 Schematic diagram of different spatial distribution structures of coke within SAPO-34 crystal.

nearly constant regardless of regeneration temperature or coke content, indicating that methanol, being a small molecule, diffuses freely through the catalyst. Consequently, its diffusion is unaffected by the spatial distribution of carbonaceous deposits, allowing complete conversion in the MTO reaction. In contrast, the diffusion coefficient of propane, representative of larger product molecules, varies significantly during the regeneration process (Figure 4). With increased free reaction space, propane diffusion improves, reducing mass transfer resistance. However, at equivalent coke levels, catalysts regenerated at 470°C exhibit lower diffusion coefficients—and consequently higher intragranular resistance—compared to those regenerated at 600°C. Molecular dynamics (MD) simulations have indicated that naphthalene's steric hindrance favors ethylene diffusion by limiting the mobility of larger olefins.[27] Therefore, the "tight-outside, loose-inside" coke distribution resulting from low-temperature regeneration enhances the diffusion of small molecules like ethylene, which is regarded as one of the reasons for enhanced ethylene selectivity.

3.4 | Pilot-scale experiments of MTO with low-temperature regeneration

After stability evaluation of 10 consecutive reaction–regeneration cycles in a microfluidized bed reactor (Figure S29), a pilot-scale experimental facility, consisting of a fluidized bed reactor–regenerator setup (Figure S30), was employed to further validate the proposed low-temperature regeneration strategy. As shown in Figure 5A,B, catalysts treated with air at 470°C in the regenerator demonstrated sustained complete methanol conversion and high selectivity for light olefins (~80.6%) over extended operational periods. Notably, under comparable average coke content, catalysts regenerated at 470°C achieved significantly higher ethylene selectivity compared to those regenerated at 600°C (Figure 5C). This finding highlights the effectiveness of the strategy for optimizing coke distribution in circulating flow reaction systems. However, it is important to note that the circulating catalysts exhibit a specific coke distribution, which remains a contributing factor in this context.

To further assess the implications of reduced regenerator temperatures on heat utilization, the regeneration system and waste heat recovery system of an industrial-scale MTO process (Figure S31) were simulated using the exergy analysis method (Supplementary Note 1.3). Three scenarios were considered: partial regeneration with residual coke contents of 3% and 8%, and complete regeneration, performed at 470 and 600°C. As shown in Table S3, high-temperature regeneration consistently produces higher levels of CO, facilitating the generation of greater quantities of superheated steam. In contrast, low-temperature regeneration primarily yields saturated steam. This distinction in heat utilization is visually represented in the system's exergy flow (Figure S33): low-temperature regeneration favors saturated steam production, while high-temperature regeneration supports superheated steam generation. Interestingly, as the residual coke content increases—indicating a higher degree of incomplete regeneration—the overall exergy efficiency of the regeneration process improves (Figure 5D). Moreover, the low-temperature regeneration method exhibits superior energy efficiency, reflecting a more effective

utilization of energy resources. These simulation results align with the observed correlation between ethylene selectivity and residual coke content, confirming that air regeneration at 470°C is a more efficient and effective approach for the MTO process.

4 | CONCLUSION

In industrial zeolite-catalyzed processes, the air regeneration strategy at high temperatures over 650°C has been traditionally implemented, aiming to restore catalyst activity while ensuring stable and continuous operations. Air combustion of coke species at such a high temperature would influence hydrothermal stability and ultimately shorten the lifetime of the catalyst. In this study, we demonstrate that a low-temperature air regeneration (440–500°C) strategy can be successfully applied to SAPO-34 catalyzed MTO process. It can strategically modulate the spatial architecture of residual coke, generating a "tight-outside, loose-inside" configuration that balances effective coke removal with catalyst preservation (Scheme 1). This unique spatial pattern promotes naphthalene exposure, enhances methanol conversion, and selectively favors ethylene formation. Unlike conventional high-temperature regeneration practices that rely on indiscriminate air combustion, this approach leverages the temperature-tuned oxidation capacity of air to selectively restructure carbonaceous deposits at the microscale, preserving key active intermediates while reopening transport pathways. The convergence of spatial coke engineering and selective oxidation chemistry underscores a powerful conceptual shift from mere coke elimination to rational coke modulation in zeolite catalysis. Pilot-scale experiments confirmed the long-term stability and enhanced olefins selectivity of the regenerated catalysts, while process simulations revealed higher exergy efficiency under low-temperature conditions. Together, these findings not only highlight the industrial viability of this regeneration strategy, but also contribute to the fundamental understanding of how spatially confined carbon species can be harnessed to direct reaction selectivity in microporous materials. This work thus offers a mechanistic framework for spatially guided regeneration in shape-selective catalysis, bridging the gap between fundamental coke chemistry and applied process design.

AUTHOR CONTRIBUTIONS

GL carried out the main experimental work, including catalytic tests and characterization, and drafted the manuscript. **JZ** conducted the pilot-scale experiments and provided key conceptual guidance for the study. **SL** and **YW** performed the isotope-labeling experiments and related analyses. **YS** and **HL** contributed significantly to the analysis and interpretation of the diffusion-related data. **HW** and **ZX** were responsible for SIM imaging and data processing. **MY** conceived and supervised the research in detail, offering critical revisions and guidance throughout the writing process. **ZL** supervised the overall execution of the project. **YS, HL** and **WP** contributed significantly to the analysis and interpretation of the diffusion-related data.

ACKNOWLEDGMENTS

This work was supported by the National Natural Science Foundation of China (No. 22293021 and 22288101).

CONFLICT OF INTEREST STATEMENT

The author declares that he has no known competing financial interests or personal relationships that could have appeared to influence the work reported in this article.

DATA AVAILABILITY STATEMENT

All numerical data from the microfluidized bed experiments used to evaluate the MTO reaction performance are compiled in DATA-S1 of Supporting Information S1 and are presented graphically in Figures 1, S4–S11, and S29. Extensive mass spectrometry data generated in this study—including qualitative analyses (Figures 3D, S13, S18, and S22), quantitative measurements (Figures 2A–C, S12, S14, S23, and S26), and isotope labeling experiments (Figures 3B,E,G,H, S24, and S25)—are provided in DATA-S2 of Supporting Information S1. All numerical results from various characterization techniques, including Raman spectroscopy (Figures 2D,E and S15–S17), SIM (Figures 2J–M and S19), *in situ* DRIFT spectroscopy (Figure 3C,F), physical adsorption (Figures 3A and S20), XRD (Figure S1), TGA (Figure S3), and IGA (Figures 4, S27, and S28), are listed in DATA-S3 of Supporting Information S1. Data from the pilot-scale experiments (Figures 5A,B,C and S30) and process simulations (Figures 5D, S32 and S33) are available in DATA-S4 of Supporting Information S1.

ORCID

Mao Ye https://orcid.org/0000-0002-7078-2402

REFERENCES

1. Smit B, Maesen TLM. Towards a molecular understanding of shape selectivity. *Nature*. 2008;451(7179):671-678. doi:10.1038/nature06552
2. Pérez-Ramírez J, Christensen CH, Egeblad K, Christensen CH, Groen JC. Hierarchical zeolites: enhanced utilisation of microporous crystals in catalysis by advances in materials design. *Chem Soc Rev*. 2008;37(11):2530-2542. doi:10.1039/b809030k
3. Olsbye U, Svelle S, Bjørgen M, et al. Conversion of methanol to hydrocarbons: how zeolite cavity and pore size controls product selectivity. *Angew Chem Int Ed*. 2012;51(24):5810-5831. doi:10.1002/anie.201103657
4. Buurmans ILC, Ruiz-Martínez J, Knowles WV, et al. Catalytic activity in individual cracking catalyst particles imaged throughout different life stages by selective staining. *Nat Chem*. 2011;3(11):862-867. doi:10.1038/nchem.1148
5. Ibarra Á, Veloso A, Bilbao J, Arandes JM, Castaño P. Dual coke deactivation pathways during the catalytic cracking of raw bio-oil and vacuum gasoil in FCC conditions. *Appl Catal Environ*. 2016;182:336-346. doi:10.1016/j.apcatb.2015.09.044
6. Dai W, Wu G, Li L, Guan N, Hunger M. Mechanisms of the deactivation of SAPO-34 materials with different crystal sizes applied as MTO catalysts. *ACS Catal*. 2013;3(4):588-596. doi:10.1021/cs400007v
7. Chen J, Li J, Wei Y, et al. Spatial confinement effects of cage-type SAPO molecular sieves on product distribution and coke formation in methanol-to-olefin reaction. *Catal Commun*. 2014;46:36-40. doi:10.1016/j.catcom.2013.11.016
8. Schmidt JE, Poplawsky JD, Mazumder B, et al. Coke formation in a zeolite crystal during the methanol-to-hydrocarbons reaction as studied with atom probe tomography. *Angew Chem Int Ed*. 2016;55(37):11173-11177. doi:10.1002/anie.201606099
9. Zhou J, Zhao J, Zhang J, Zhang T, Ye M, Liu Z. Regeneration of catalysts deactivated by coke deposition: a review. *Chin J Catal*. 2020;41(7):1048-1061. doi:10.1016/S1872-2067(20)63552-5

10. Zhang H, Shen Z, Gong J, Liu H. Influences of regeneration atmospheres on structural transformation and renderability of fluidized catalytic cracking catalyst. *Chin J Chem Eng*. 2023;63:71-80. doi:10.1016/j.cjche.2023.04.020
11. Akbari A, Haji Andevary H, Omidkhah M. Boosted regeneration of coked SAPO-34 catalyst in MTO fluidized bed reactor by diluted air at elevated temperatures. *Chem Eng Process-Process Intensif*. 2024;201:109821. doi:10.1016/j.cep.2024.109821
12. Tian P, Wei Y, Ye M, Liu Z. Methanol to olefins (MTO): from fundamentals to commercialization. *ACS Catal*. 2015;5(3):1922-1938. doi:10.1021/acscatal.5b00007
13. Sun T, Xu S, Xiao D, et al. Water-induced structural dynamic process in molecular sieves under mild hydrothermal conditions: ship-in-a-bottle strategy for acidity identification and catalyst modification. *Angew Chem Int Ed*. 2020;59(46):20672-20681. doi:10.1002/anie.202009648
14. Yang L, Wang C, Zhang L, et al. Stabilizing the framework of SAPO-34 zeolite toward long-term methanol-to-olefins conversion. *Nat Commun*. 2021;12(1):4661. doi:10.1038/s41467-021-24403-2
15. Li Z, Martínez-Triguero J, Yu J, Corma A. Conversion of methanol to olefins: stabilization of nanosized SAPO-34 by hydrothermal treatment. *J Catal*. 2015;329:379-388. doi:10.1016/j.jcat.2015.05.025
16. Campbell SM, Bibby DM, Coddington JM, Howe RF. Dealumination of HZSM-5 zeolites. II. Methanol to gasoline conversion. *J Catal*. 1996;161:350-358.
17. Almutairi SMT, Mezari B, Pidko EA, Magusin PCMM, Hensen EJM. Influence of steaming on the acidity and the methanol conversion reaction of HZSM-5 zeolite. *J Catal*. 2013;307:194-203. doi:10.1016/j.jcat.2013.07.021
18. Wang C, Aztiria T, Rzepka P, et al. Structural changes of ZSM-5 catalysts during methanol-to-hydrocarbons conversion processes. *ACS Catal*. 2024;14(16):12410-12424. doi:10.1021/acscatal.4c02625
19. Yarulina I, Chowdhury AD, Meirer F, Weckhuysen BM, Gascon J. Recent trends and fundamental insights in the methanol-to-hydrocarbons process. *Nat Catal*. 2018;1(6):398-411. doi:10.1038/s41929-018-0078-5
20. Lin S, Zhi Y, Chen W, et al. Molecular routes of dynamic autocatalysis for methanol-to-hydrocarbons reaction. *J Am Chem Soc*. 2021;143(31):12038-12052. doi:10.1021/jacs.1c03475
21. Chen D, Rebo HP, Moljord K, Holmen A. Influence of coke deposition on selectivity in zeolite catalysis. *Ind Eng Chem Res*. 1997;36(9):3473-3479. doi:10.1021/ie9700223
22. Hereijgers BPC, Bleken F, Nilsen MH, et al. Product shape selectivity dominates the methanol-to-olefins (MTO) reaction over H-SAPO-34 catalysts. *J Catal*. 2009;264(1):77-87. doi:10.1016/j.jcat.2009.03.009
23. Zhong J, Han J, Wei Y, Liu Z. Catalysts and shape selective catalysis in the methanol-to-olefin (MTO) reaction. *J Catal*. 2021;396:23-31. doi:10.1016/j.jcat.2021.01.027
24. Han J, Liu Z, Li H, et al. Simultaneous evaluation of reaction and diffusion over molecular sieves for shape-selective catalysis. *ACS Catal*. 2020;10(15):8727-8735. doi:10.1021/acscatal.0c02054
25. Zhou J, Zhi Y, Zhang J, et al. Presituated "coke"-determined mechanistic route for ethene formation in the methanol-to-olefins process on SAPO-34 catalyst. *J Catal*. 2019;377:153-162. doi:10.1016/j.jcat.2019.06.014
26. Zhou J, Zhang J, Zhi Y, et al. Partial regeneration of the spent SAPO-34 catalyst in the methanol-to-olefins process via steam gasification. *Ind Eng Chem Res*. 2018;57(51):17338-17347. doi:10.1021/acs.iecr.8b04181
27. Zhou J, Gao M, Zhang J, et al. Directed transforming of coke to active intermediates in methanol-to-olefins catalyst to boost light olefins selectivity. *Nat Commun*. 2021;12(1):17. doi:10.1038/s41467-020-20193-1
28. Wang C, Yang L, Gao M, et al. Directional construction of active naphthalenic species within SAPO-34 crystals toward more efficient methanol-to-olefin conversion. *J Am Chem Soc*. 2022;144(46):21408-21416. doi:10.1021/jacs.2c10495
29. Lin S, Zhi Y, Zhang W, et al. Hydrogen transfer reaction contributes to the dynamic evolution of zeolite-catalyzed methanol and dimethyl ether conversions: insight into formaldehyde. *Chin J Catal*. 2023;46:11-27. doi:10.1016/S1872-2067(22)64194-9
30. Lezcano-Gonzalez I, Campbell E, Hoffman AEJ, et al. Insight into the effects of confined hydrocarbon species on the lifetime of methanol conversion catalysts. *Nat Mater*. 2020;19(10):1081-1087. doi:10.1038/s41563-020-0800-y
31. An H, Zhang F, Guan Z, Liu X, Fan F, Li C. Investigating the coke formation mechanism of H-ZSM-5 during methanol dehydration using operando UV–Raman spectroscopy. *ACS Catal*. 2018;8(10):9207-9215. doi:10.1021/acscatal.8b00928
32. Campbell E, Sazanovich IV, Towrie M, Watson MJ, Lezcano-Gonzalez I, Beale AM. Methanol-to-olefins studied by UV Raman spectroscopy as compared to visible wavelength: capitalization on resonance enhancement. *J Phys Chem Lett*. 2024;15(26):6826-6834. doi:10.1021/acs.jpclett.4c00865
33. Wang N, Wang L, Zhi Y, et al. Coking and decoking chemistry for resource utilization of polycyclic aromatic hydrocarbons (PAHs) and low-carbon process. *J Energy Chem*. 2023;76:105-116. doi:10.1016/j.jechem.2022.09.014
34. Van Vreeswijk SH, Parker LA, Sanderse AT, Oord R, Meirer F, Weckhuysen BM. Utilizing operando catalyst regeneration to uncover insights in the methanol-to-hydrocarbons process. *Chem Catal*. 2024;4:101134. doi:10.1016/j.checat.2024.101134
35. Gao M, Li H, Liu W, et al. Imaging spatiotemporal evolution of molecules and active sites in zeolite catalyst during methanol-to-olefins reaction. *Nat Commun*. 2020;11(1):3641. doi:10.1038/s41467-020-17355-6
36. Lin S, Zhi Y, Liu Z, et al. Multiscale dynamical cross-talk in zeolite-catalyzed methanol and dimethyl ether conversions. *Natl Sci Rev*. 2022;9(9):nwac151. doi:10.1093/nsr/nwac151
37. Park JW, Seo G. IR study on methanol-to-olefin reaction over zeolites with different pore structures and acidities. *Appl Catal A: Gen*. 2009;356(2):180-188. doi:10.1016/j.apcata.2009.01.001
38. Qian Q, Vogt C, Mokhtar M, et al. Combined operando UV/Vis/IR spectroscopy reveals the role of methoxy and aromatic species during the methanol-to-olefins reaction over H-SAPO-34. *ChemCatChem*. 2014;6(12):3396-3408. doi:10.1002/cctc.201402714
39. Goetze J, Meirer F, Yarulina I, et al. Insights into the activity and deactivation of the methanol-to-olefins process over different small-pore zeolites As studied with operando UV–vis spectroscopy. *ACS Catal*. 2017;7:4033-4046.
40. Cnudde P, Demuynck R, Vandenbrande S, Waroquier M, Sastre G, Speybroeck VV. Light olefin diffusion during the MTO process on H-SAPO-34: a complex interplay of molecular factors. *J Am Chem Soc*. 2020;142(13):6007-6017. doi:10.1021/jacs.9b10249

SUPPORTING INFORMATION

Additional supporting information can be found online in the Supporting Information section at the end of this article.

How to cite this article: Li G, Zhang J, Lin S, et al. Harnessing structured coke in zeolites to boost ethylene yield in methanol-to-olefins by low-temperature regeneration. *AIChE J*. 2025;71(12):e70083. doi:10.1002/aic.70083